Role of MgCo compound on the sorption properties of the Mg–Co milled mixtures

M.G. Verón[a], F.C. Gennari[a,b,*], G.O. Meyer[a,b]

[a] Instituto Balseiro (UNCuyo and CNEA), S.C. de Bariloche, Argentina
[b] Consejo Nacional de Investigaciones Científicas y Técnicas (CONICET), Instituto Balseiro (Universidad Nacional de Cuyo), Centro Atómico Bariloche, 8400 S.C. de Bariloche, Argentina

ARTICLE INFO

ABSTRACT

The influence of MgCo on the reaction paths during hydriding and dehydriding processes of Mg–Co mixtures was studied using a combined HP-DSC and XRD approach. Mg–Co mixtures with different compositions were mechanically milled under argon to prepare Mg–Co nanocomposites and then submitted to thermal treatment at 300 °C for 5 days to induce MgCo formation. The local Mg–Co composition in the milled and milled-heated samples determines the nature of the phases obtained after hydriding/dehydriding cycling. The formation of $Mg_6Co_2H_{11}$, Mg_2CoH_5 and MgH_2 hydrides occurs after the first hydriding stage of the 2Mg–Co and Mg–Co milled mixtures due to kinetic restrictions. On the contrary, Mg–Co milled-heated mixture exhibits the selective formation of Mg_2CoH_5 during first hydriding via two-step reaction. In the first one, MgCo disproportion to MgH_2 and Co takes place simultaneously with Mg hydriding (<200 °C). The second step involves MgCo hydriding to Mg_2CoH_5 through MgH_2 as intermediate phase (>200 °C). Dehydriding reaction is enhanced by dispersion of Co into Mg-matrix, which reduces more than 100 °C the hydrogen desorption temperature when compared with the Mg–Co milled sample without previous heating.

© 2009 Elsevier B.V. All rights reserved.

1. Introduction

Hydrogen is considered the most promising and cleanest energy carrier to replace fossil fuels. However, one of the challenges for its application in a zero-emission vehicle is to develop a safe and economic hydrogen storage medium. Research in many laboratories around the world has focused on solid-state hydrogen storage materials. Among the materials under consideration magnesium (theoretically 7.6 wt% of hydrogen storage capacity) and transition metal complex hydrides of the family $MgTH_y$ (T = Fe, Co, Ni) (5.5 wt.%, 4.5 wt.% and 3.6 wt.%, respectively) are attractive because of their high theoretical capacity, high volumetric densities of hydrogen (between 80 and 150 kg H_2 m^{-3}) and low cost [1]. However, single-phase hydrides of this family are not easy to produce mainly because the absence of a precursor alloy such as Mg_2Co or Mg_2Fe, the large difference between melting points of the metals, and the high vapor pressure of magnesium [2–4]. As a consequence, their syntheses present important problems to resolve [3–12].

Mechanical milling is a synthesis technique used to prepare nanocrystalline materials that overcomes several limitations mentioned before. It favors the formation of special microstructures, improves transition metal dispersion, modifies surface characteristics and reduces particle size, which has a favorably influence on hydrogen sorption properties. Our group has successfully obtained transition metal complex hydrides (Fe, Co, Ni) using mechanical milling combined with sintering or reactive mechanical milling [13–20]. Due to the fact that the properties of reaction with hydrogen are very sensitive to microstructural modifications introduced during milling, enhanced hydrogenation behavior were observed for Mg_2FeH_6, Mg_2CoH_5 and Mg_2NiH_4. However, a more general understanding of the role of Mg–Co–H and Mg–Fe–H reaction intermediates for the complex hydride formation has not yet been established.

In particular, the Mg–Co–H system is interesting *per se*: different hydride phases can be observed as a function of temperature, pressure and time, such as tetragonal β-Mg_2CoH_5, orthorhombic γ-Mg_3CoH_5 and tetragonal β-MgH_2 [3,5,7]. The disorder structure of γ-Mg_3CoH_5 was further determined as orthorhombic with a composition equal to $Mg_6Co_2H_{11}$ [6]. Moreover, a reversible structural transformation is observed with temperature: tetragonal β-Mg_2CoH_5 transforms into a disordered cubic modification at 215 °C [3,5]. In addition, the only one stable intermetallic compound reported in the Mg–Co phase diagram is $MgCo_2$ [2], i.e. there are no stable precursors such as Mg_2Co or Mg_3Co to produce a single hydride. However, evaluation of Mg–Co thermodynamic information available in the literature has demonstrated the existence of $Mg_{2-x}Co$ compound in the Mg-rich zone [5,9,12,21,22].

* Corresponding author at: Consejo Nacional de Investigaciones Científicas y Técnicas (CONICET), Instituto Balseiro (Universidad Nacional de Cuyo), Centro Atómico Bariloche, 8400 S.C. de Bariloche, Argentina. Tel.: +54 2944 445118; fax: +54 2944 445190.
E-mail address: gennari@cab.cnea.gov.ar (F.C. Gennari).

Recently, the formation of an intermetallic between Mg–Co with a composition MgCo has been demonstrated [21,22]. It was obtained by solid-state reaction of Mg–Co mixtures (reaction (1)) or during the β-Mg$_2$CoH$_5$ decomposition (reaction (2)) [5,9,12,18,21,22]. The formation reactions can be represented as:

$$Mg(s) + Co(s) \rightarrow MgCo(s) \tag{1}$$

$$Mg_2CoH_5(s) \rightarrow MgCo(s) + Mg(s) + 5/2H_2(g) \tag{2}$$
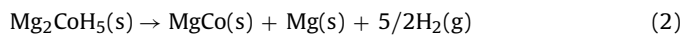
Although systematic studies of the factors that influence both reactions have not been performed, they seem to be mainly function of temperature: MgCo was not observed after decomposition of Mg$_2$CoH$_5$ at 350 °C but it was formed if the same sample is heated up to 450 °C [18]. Therefore, thermally activated diffusion of Co into Mg could be necessary to favor the MgCo formation. How the presence of MgCo intermetallic compound influences the formation of different hydrides and their hydriding/dehydriding kinetics remains unknown. In particular, there is a lack of experimental evidence of reversibility of reaction (2) and analysis for the reaction path. It is of both practical importance and scientific interest to elucidate the role of MgCo presence on the reaction of Mg–Co mixtures with hydrogen.

In this paper, we investigate the effect of MgCo phase on the reactivity of Mg–Co mixtures and the nature of the hydride phases through measurement of hydrogenation/dehydrogenation reactions. Combination of high pressure differential scanning calorimetry (HP-DSC) and X-ray diffraction (XRD) techniques showed that MgCo can be rehydrogenated at 400 °C under 2 MPa of hydrogen pressure. During hydriding of MgCo, the formation of Mg$_2$CoH$_5$ is favored over other potential hydride phases. Possible mechanisms of hydrogenation and dehydrogenation reactions are discussed below.

2. Experimental

2.1. Material synthesis

Powders of Mg and Co (purity higher than 99.9%) were used to perform mechanical milling (MM) using a Uni-Ball-Mill II apparatus (Australian Scientific Instruments) with an external magnetic field controlling the ball movement. Mg–Co mixtures of 1:1 and 2:1 relative composition were milled under argon during 200 h using ferromagnetic steel balls as milling media into a stainless steel container. The final samples are hereafter indicated as 1M and 2M, respectively. Ball-to-powder weight ratio was 44:1. All handling was performed in a glove box under purified argon atmosphere.

As-milled samples were placed in an aluminum capsule and hermetically closed in a dry glove box. After this, the aluminum capsules were placed in quartz tube and outgassed in vacuum (10^{-2} Pa) for half an hour at room temperature. Then, the tubes were sealed and heated up to 300 °C during 5 days (samples labeled 1M and 2M). After that, the aluminum capsules were recovered by breaking the quartz tube at room temperature under air atmosphere. Hereafter these samples are named 1MH and 2MH, in correlation with Mg–Co compositions 1:1 and 2:1, respectively.

2.2. High pressure-differential scanning calorimetry (HP-DSC) and XRD approach

Differential scanning calorimetric were performed with a HP-DSC equipment (TA Instrument 2910) on samples of 0.03 g of loaded into aluminum capsules hermetically closed in a glove box under purified argon atmosphere. Hydride phase content was estimated from DSC curves using the peak area and the mass of each sample. To investigate the stages and hydride phases present during hydro-

gen absorption/desorption reactions the following procedure were performed into HP-DSC equipment:

(1) First absorption: sample was heated under 2.0 MPa of hydrogen from room temperature to 300 °C (400 °C) and then kept at this temperature for 1 h (0.5 h).
(2) First desorption: sample was heated from room temperature to 400 °C under vacuum and kept at this temperature for 0.5 h.
(3) Second absorption: sample was heated under 2.0 MPa of hydrogen from room temperature to 300 °C (400 °C) and then kept at this temperature for 1 h (0.5 h).

Crystalline structure of as-milled, as-heated and hydrided/dehydrided samples powders was characterized by XRD analysis on a Philips PW 1710/01 Instruments with CuKα radiation (graphite monochromator).

2.3. Microstructural and hydrogen sorption characterizations

The agglomerate microstructure and Co distribution were characterized by scanning electron microscopy (SEM 515, Philips Electronic Instruments) on resin-mounted and polished samples. Isothermal hydrogen sorption curves were obtained using a modified Sieverts-type equipment, coupled with a mass flow controller [23]. Hydrogen absorption/desorption rates were measured at 250–350 °C and 2.0 MPa following two different procedures: in one of them the sample was heated at 400 °C for 1 h and then cooled to 250–350 °C and kept at this temperature for 30 min before observing its absorption/desorption reaction with hydrogen. In the other procedure, the resulting sample was submitted to an absorption/desorption cycle at 250–350 °C without being heated at 400 °C.

3. Results and discussions

3.1. Formation of MgCo intermetallic from Mg–Co mixtures by solid-state reaction

Fig. 1A and C show the XRD patterns of the Mg–Co mixtures 2M and 1M after ball milling, in which the peaks of Co and Mg are indicated. Neither new phases nor reactions can be observed
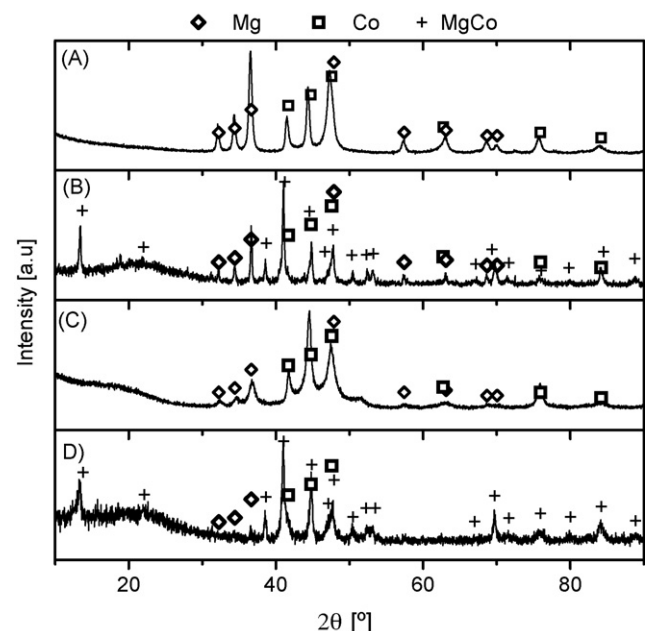

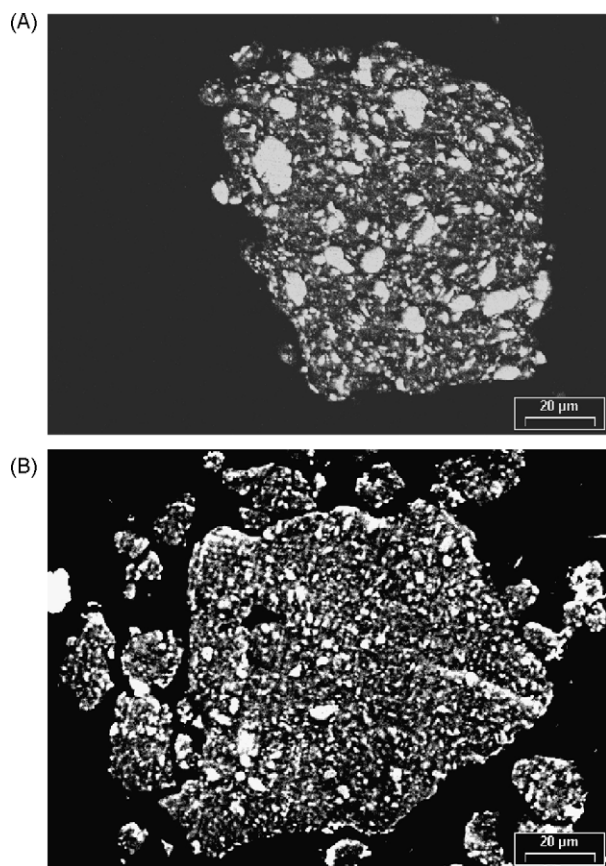**Fig. 1.** X-ray diffraction patterns of: (A) 2M, (B) 2MH, (C) 1M and (D) 1MH samples.

Fig. 2. SEM backscattered electron images of (A) 2M and (B) 1M samples after 200 h of milling under argon.

Fig. 3. HP-DSC curves during first and second hydrogen absorption reaction cycles for (A) 2M and (B) 2MH samples (heating rate 5 °C min^{-1} and 2 MPa of H$_2$ pressure). (C) HP-DSC curves during first hydrogen desorption for 2M and 2MH samples (heating rate 5 °C min^{-1} under vacuum).

after 200 h of milling. The average crystallite sizes were progressively reduced from microns to nanometer order of magnitude. Final crystallite sizes were 20 (10) nm and 22(15) nm for Mg and Co, respectively, in 2M (1M) sample. Heating as-milled samples at 300 °C for 5 days developed new phases (Fig. 1B and D). The new peaks were attributed to cubic MgCo, in accordance with previous works [21]. Up to now, this is the lower temperature reported for the formation of MgCo intermetalic *via* solid-state reaction. Phase abundance depends on Mg–Co composition. For the sample with 1:1 Mg–Co ratio, the amount of free Mg and Co was practically undetectable by XRD, whereas for that with 2:1 ratio both Co and Mg peaks were clearly identified. The higher reactivity of the 1:1 mixture could be a consequence of a greater contact between Mg and Co (see Fig. 2), in agreement with previous results [22].

Co distribution into the Mg matrix was analyzed for 2M and 1M Mg–Co mixtures by SEM (backscattered electrons). Fig. 2A and B show Co particles (brightest phase) dispersed into Mg matrix (darkest phase). The best intermixing reached by ball milling under Ar was observed after 200 h of processing, due to a combination of
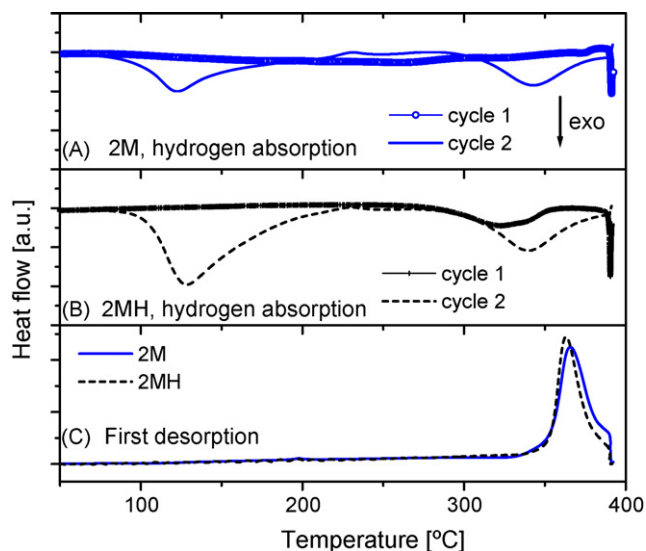
fracturing and cold welding mechanisms which produce the refinement of the microstructure and a uniform dispersion of the Co particles within the magnesium matrix. The size of the starting Co particles was reduced to less than 10 μm.

3.2. Hydrogen reactivity of 2Mg–Co mixture: MgCo as intermediate for Mg$_2$CoH$_5$ formation

In order to investigate the reactivity of 2M and 2MH samples with hydrogen, absorption/desorption cycles were performed. HP-DSC curves obtained are shown in Fig. 3. First hydrogen absorption from 2M sample (Fig. 3A) is considered an activation process, as can be inferred from the broad exothermic peak starting at 130 °C [24]. For 2MH sample (Fig. 3B) hydrogen absorption started at higher temperature (250 °C) in comparison with 2M sample, but total hydrogen content was higher probably due to partial activation during pre-heating at 300 °C. Moreover, in the second cycle both samples showed two sharp exothermic peaks involving higher hydrogen storage than first cycle. The maximum amount of hydrogen absorbed was observed for 2MH after second cycle, being 1.5 times that of 2M. On the other hand, first desorption cycle started at about 330 °C for 2M and 2MH samples (Fig. 3C), independently of previous hydrogen absorption behavior observed.

To clarify the reaction paths involved during absorption/desorption reaction, XRD analyses were performed after each cycle. The phases detected at different temperatures and after different absorption/desorption cycles are summarized in Table 1. It can be seen that first absorption cycle for 2M sample leads to the formation of Mg$_6$Co$_2$H$_{11}$ as the main phase up to 300 °C, whereas

Table 1
XRD analysis performed on the 2M and 2MH samples after different thermal treatments.

Sample	Cycle	Final temperature (°C) and time (h)	Phases detected by XRD[*]
2M	Absorption 1	300 °C, 0 h	**Mg$_6$Co$_2$H$_{11}$**≈**MgH$_2$**/Mg/Co
	Absorption 1	400 °C, 0.5 h	**Mg$_6$Co$_2$H$_{11}$**/MgH$_2$/Mg$_2$CoH$_5$/Mg/Co
	Desorption 1	400 °C, 0.5 h	MgCo/Mg/Co
	Absorption 2	400 °C, 0.5 h	**Mg$_2$CoH$_5$**/Mg$_6$Co$_2$H$_{11}$/MgH$_2$/Co
2MH	Absorption 1	400 °C, 0.5 h	**Mg$_6$Co$_2$H$_{11}$** ≈**Mg$_2$CoH$_5$**/MgH$_2$/Co
	Desorption 1	400 °C, 0.5 h	MgCo/Mg/Co
	Absorption 2	400 °C, 0.5 h	**Mg$_2$CoH$_5$**/MgH$_2$/Co

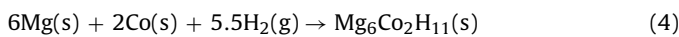[*] The main hydride phase is indicated in bold letters.

Table 2
XRD analysis performed on the 2M sample after different thermal treatments.

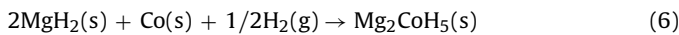| Cycle	Final temperature (°C) and time (h)	Phases detected by XRD[*]
Absorption 1	300 °C, 1 h	**$Mg_6Co_2H_{11}$**/MgH_2/Mg/Co
Desorption 1	400 °C, 0.5 h	$MgCo$/Mg/Co
Absorption 2	300 °C, 1 h	$Mg_6Co_2H_{11}$/**MgH_2**/Mg_2CoH_5/Mg/Co/$MgCo$
Absorption 1	300 °C, 1 h	**$Mg_6Co_2H_{11}$**/MgH_2/Mg/Co
Desorption 1	400 °C, 0 h	Mg/Co
Absorption 2	300 °C, 1 h	**$Mg_6Co_2H_{11}$**/MgH_2/Mg/Co

[*] The main hydride phase is indicated in bold letters.

Mg_2CoH_5 was observed at high temperature (400 °C). Moreover, after second hydriding cycle Mg_2CoH_5 formation was favored over other hydrides phases. The main reactions occurring during first absorption cycle of 2M sample can be represented:

Temperature < 300 °C

$$Mg(s) + H_2(g) \rightarrow MgH_2(s) \tag{3}$$

$$6Mg(s) + 2Co(s) + 5.5H_2(g) \rightarrow Mg_6Co_2H_{11}(s) \tag{4}$$

Temperature > 300 °C

$$2Mg(s) + Co(s) + 5/2H_2(g) \rightarrow Mg_2CoH_5(s) \tag{5}$$

$$2MgH_2(s) + Co(s) + 1/2H_2(g) \rightarrow Mg_2CoH_5(s) \tag{6}$$

It is interesting to note that MgCo was obtained when desorption process was performed up to 400 °C and kept at this temperature for 0.5 h. The presence of MgCo at the beginning of the second absorption cycle suggests that this compound is an intermediate phase for the formation of Mg_2CoH_5 under cycling according to

$$MgCo(s) + Mg(s) + 5/2H_2(g) \rightarrow Mg_2CoH_5(s) \tag{2}$$
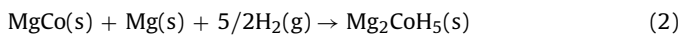
Similar evidence was obtained from hydrogen cycling of 2MH sample: MgCo compound was presented in the starting sample and favored the formation of Mg_2CoH_5 during first cycle (Table 1). For 2MH, additional formation of $Mg_6Co_2H_{11}$ was possible due to the presence of free Co and Mg (Fig. 1C). Hence, both the change in the thermal behavior observed from the first to second absorption cycle as well as the trends to the formation of Mg_2CoH_5 with cycling evidence that the 2MH sample was not completely activated during pre-heating at 300 °C for 5 days.

To understand the role of MgCo on the formation of Mg_2CoH_5, two hydrogen absorption procedures for 2M sample were performed heating up to 300 °C, with an intermediate desorption step up to 400 °C. In one of the desorption procedures, the sample was heated up to 400 °C and kept at this temperature during 0.5 h to induce MgCo formation. In the other case the sample was continuously heated up to 400 °C and then cooled down. Table 2 summarizes the phases detected after absorption/desorption cycles. From the analysis of the phases observed after each cycle, three important conclusions could be inferred. The most important remark was that MgCo production during desorption stage was responsible of the enhanced Mg_2CoH_5 formation at 300 °C observed after the second hydriding step. Additional conversion of MgCo into Mg_2CoH_5 according reaction (2) was possible at high temperature, as solid–solid diffusion processes were enhanced. Moreover, MgCo formation was due to the solid–solid reaction between Mg and Co obtained from $Mg_6Co_2H_{11}$/Mg_2CoH_5 decomposition. To allow enough MgCo formation this reaction required the sample to be heated some time (0.5 h) at 400 °C.

It was also observed that kinetics restrictions limit $Mg_6Co_2H_{11}$ formation during the first cycle, being associated with Co availability in Mg neighborhood. Homogenization of 2Mg–Co composition sample was reached after additional heating up to 400 °C during absorption/desorption cycling. Then, local Mg:Co composition was

modified after the first absorption stage, reaching a 2:1 distribution that facilitated Mg_2CoH_5 formation via MgCo intermediate compound (Table 1). Mg_2CoH_5 as unique hydride of 2MH sample after second hydriding cycle reinforces this hypothesis.

3.3. Reversibility between MgCo/Mg$_2$CoH$_5$ during absorption/desorption cycles

The above study for the 2Mg:Co system shows that hydriding and dehydriding cycling leads to multiple interactions with the subsequent formation of hydride mixtures. In order to investigate experimentally the reversibility of reaction (2), a 1:1 Mg–Co milled (1M) and another milled and heated (1MH) samples were in-situ hydrided/dehydrided with the HP-DSC technique. Fig. 4A–C shows the absorption/desorption HP-DSC profiles obtained for both samples. During first absorption stage of 1M sample, two broad exothermic peaks were observed suggesting that hydriding reaction occurred in two-steps. Second absorption showed again two-step hydrogen absorption, but the exothermic peaks were sharper and involved about 2.7 times more heat flow than during the first cycle. As it was observed for 2M sample, first hydrogen absorption should be considered as an activation-homogenization step, where Co diffusion into Mg was improved [23]. On the other hand, the first hydrogen absorption of 1MH sample showed two sharp exothermic peaks, the same it was observed in 1M sample. This behavior was ascribed to previous thermal activation of the sample which produced homogenization of the Mg–Co composition and MgCo formation: in the first hydrogen absorption of 1MH sample (Fig. 1D) or in the second of 1M sample. An analysis based on XRD results will be showed below.

In order to identify each reaction step during hydriding/dehydriding, XRD analysis were carried out and the results are summarized in Table 3. Fig. 5 compares the XRD patterns of 1M sample hydrided and dehydrided. After first absorption stage a mixture of Mg_2CoH_5–$Mg_6Co_2H_{11}$ was obtained, with Mg_2CoH_5 as main hydride phase (Fig. 5A). Hydrogen desorption favored MgCo formation with free Mg and Co (Fig. 5B). During the second absorption stage, two samples were taken out to identify the nature of the phases: one after first exothermic peak (Fig. 5C) and the other at the end of the cycle (Fig. 5D). Fig. 5C shows the presence of MgCo,
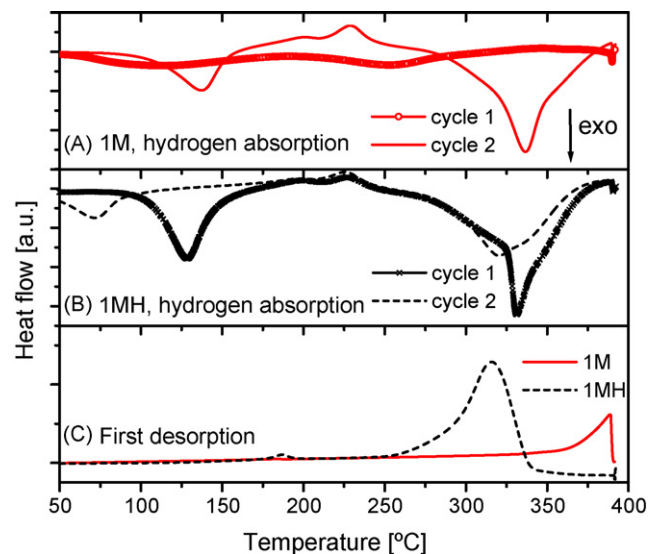

Fig. 4. HP-DSC curves during first and second hydrogen absorption reaction cycles for (A) 1M and (B) 1MH samples (heating rate 5 °C min^{-1} and 2 MPa of H$_2$ pressure). (C) HP-DSC curves during first hydrogen desorption for 1M and 1MH samples (heating rate 5 °C min^{-1} under vacuum).

Table 3
XRD analysis performed on the 1M and 1MH samples after different thermal treatments.

| Sample	Cycle	Final temperature (°C) and time (h)	Phases detected by XRD[*]
1M	Absorption 1	400 °C, 0.5 h	$Mg_6Co_2H_{11}$/**Mg_2CoH_5**/Mg/Co
	Desorption 1	400 °C, 0.5 h	MgCo/Mg/Co
	Absorption 2	190 °C, 0 h	**MgH_2**/Mg/Co/MgCo
		400 °C, 0.5 h	**Mg_2CoH_5**/Co
1MH	Absorption 1	190 °C, 0 h	**MgH_2**/Mg/Co/MgCo
	Absorption 1	400 °C, 0.5 h	**Mg_2CoH_5**/Co
	Desorption 1	400 °C, 0.5 h	MgCo/Mg/Co
	Absorption 2	400 °C, 0.5 h	**Mg_2CoH_5**/Co

[*] The main hydride phase is indicated in bold letters.

MgH_2 and Co after the first exothermic peak, whereas Mg_2CoH_5 and Co were detected at the end of the second cycle. These results evidenced the reversibility of reaction (2) and also the occurrence of the transformation of MgH_2 into Mg_2CoH_5 (reaction (6)). The origin of MgH_2 after the first exothermic peak could be ascribed to two possible reactions: hydriding of free Mg (reaction (3)) and disproportion of MgCo in the presence of hydrogen to produce MgH_2 and free Co (reaction (7)):

$$MgCo(s) + H_2(g) \rightarrow MgH_2(s) + Co(s) \qquad (7)$$
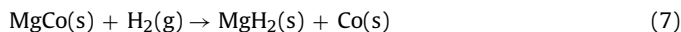
Analogous mechanisms to that proposed in Eq. (7) were found for Mg_2Cu alloy [25]. Reaction (7) was a necessary step for the formation of Mg_2CoH_5 during second exothermic peak, considering that MgH_2, MgCo and Co were the phases detected at the beginning of this stage. The absence of free Mg made difficult the extension of reaction (2). The complete reaction mechanism for Mg_2CoH_5 formation during heating from room temperature to 400 °C could be represented as:

Temperature < 200 °C (first exothermic peak)

$$Mg(s) + H_2(g) \rightarrow MgH_2(s) \qquad (3)$$

$$MgCo(s) + H_2(g) \rightarrow MgH_2(s) + Co(s) \qquad (7)$$
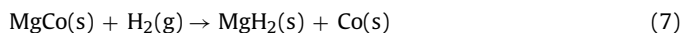
Temperature > 250 °C (second exothermic peak)

$$2MgH_2(s) + Co(s) + 1/2H_2(g) \rightarrow Mg_2CoH_5(s) \qquad (6)$$
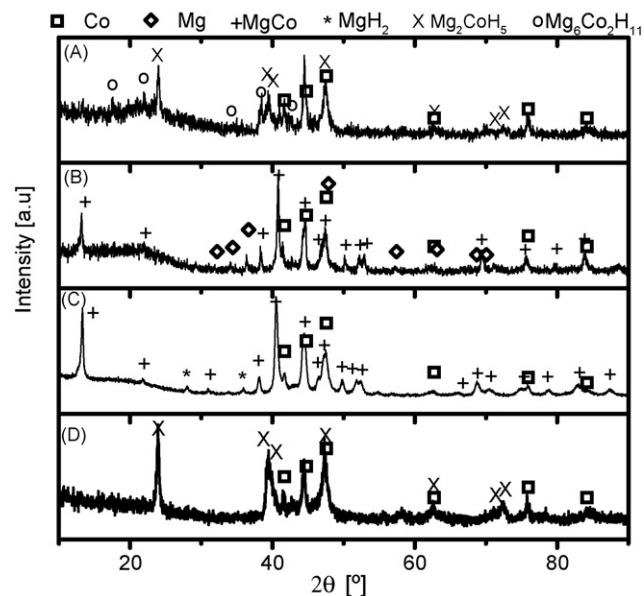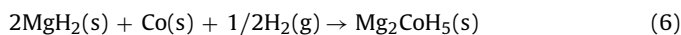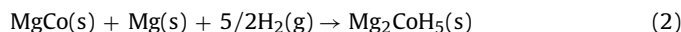

Fig. 5. X-ray diffraction patterns of 1M sample after: (A) first hydrogen absorption cycle; (B) first hydrogen desorption cycle; (C) second hydrogen absorption cycle at 200 °C; and (D) second hydrogen absorption cycle at 400 °C.

The complete reaction could be summarized as:

$$MgCo(s) + Mg(s) + 5/2H_2(g) \rightarrow Mg_2CoH_5(s) \qquad (2)$$

Therefore, Mg_2CoH_5 formation requires MgH_2 obtained from reaction (7) to allow further reaction of MgH_2 with Co (reaction (6)). Additional XRD studies performed on 1MH samples during hydriding/dehydriding cycling corroborated that the similar thermal behavior than 1M (second cycle) and 1MH samples (first cycle) was due to the same reaction path: MgH_2 formation during the first absorption peak and Mg_2CoH_5 phase growth after second exothermic peak. The above results confirmed that hydriding reaction of 1:1 Mg–Co mixture followed reaction (2), with an intermediate step involving MgH_2. Only when Mg and Co were available as free phases, alternatives reaction paths were possible.

An additional observation emerges from Fig. 4: hydrogen desorption started at about 360 °C and 250 °C, for 1M and 1MH, respectively. Then, reduction in hydrogen desorption temperature was larger than 100 °C for the sample with MgCo phase submitted to hydriding/dehydriding cycling. Moreover, we observed the peak corresponding to tetragonal-cubic Mg_2CoH_5 transformation. On the basis of XRD diffraction studies, the main difference between 1M and 1MH was the presence of MgCo in the starting sample (Fig. 1). We believe that its formation is an evidence of good Mg–Co homogenization during thermal treatment which leads to the formation of Mg_2CoH_5 as the main hydride phase during the first absorption cycle. The improved Co dispersion in the Mg-based matrix acts as catalyst for hydrogen desorption from Mg_2CoH_5 [26,27]. The thermal behavior and the phases detected after first hydriding reaction for 2M, 2MH and 1M samples showed that the first cycle was an activation process which improved homogenization of Mg–Co and Co distribution.

3.4. Effect of the MgCo formation on the absorption/desorption rate

Fig. 6 shows hydrogen absorption curves at 250 °C, 300 °C (Fig. 6A) and 350 °C (Fig. 6B) for a 2M sample without and with preheating at 400 °C for 1 h. The sample was previously activated by hydriding/dehydriding up to observe repeatability in its kinetics behavior. The hydrogen absorption content decreased with the temperature and it was dependent of the MgCo presence in the sample for 250 °C and 300 °C (Fig. 6A). During the measurements of the 2M sample without thermal treatment, Mg and Co were free to react with hydrogen via reactions (3), (4), (5) and probably also reaction (6). These reactions were favored due to both improved Mg–Co distribution and Co dispersion which acted as catalysts, when MgCo compound was not present. When the 2M sample was heated at 400 °C, free Mg and Co promoted MgCo formation so the global reaction should involve the disproportion of MgCo to MgH_2 (reaction (7)). As a consequence, 2M sample submitted to pre-heating at 400 °C showed a reduction of the total hydrogen storage capacity and a diminishing of the reaction rate.
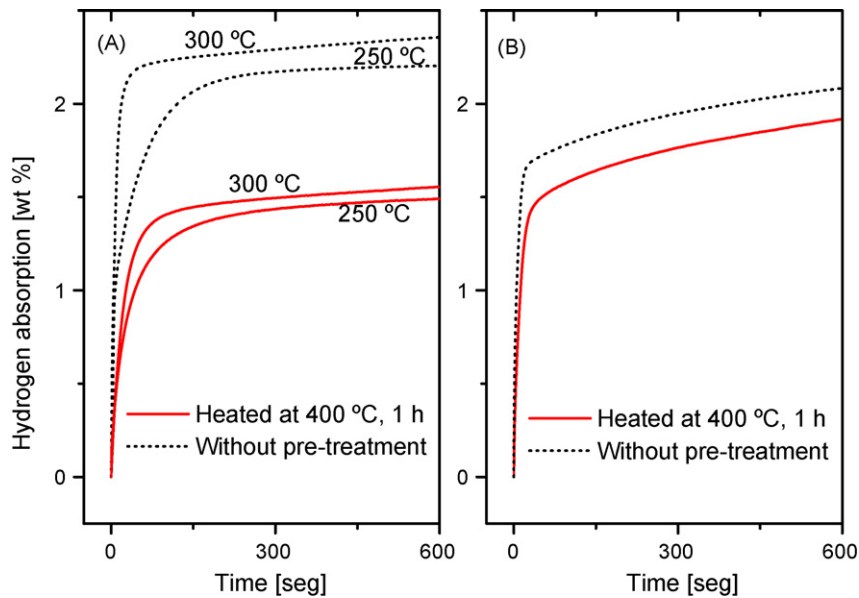
Fig. 6. Hydrogen absorption kinetics for 2M sample without and with pre-heating at 400 °C for 1 h, performed at: (A) 250 and 300 °C; (B) 350 °C. Initial pressure 2 MPa.

Therefore, global reaction rate seemed to be controlled by reaction (7), probably by some mass transport process.

Absorption curves performed at 350 °C (Fig. 6B) showed similar behavior, i.e. the absorption rate and total hydrogen content decrease for the sample submitted to thermal treatment at 400 °C. However, the difference between them was less relevant than that previously observed at 250 and 300 °C, mainly due to the fact that the occurrence of reaction (7) was favored by a temperature increase (Fig. 3). On the other hand, by comparison with the absorption experiment at 300 °C (Fig. 6A), the reaction rate is lower. It could be explained considering that Co reduced kinetics barriers at all temperatures, but thermodynamic driving force at 350 °C dominated the reaction rate and overcompensates the changes in the kinetics barriers. In particular, for measurements performed at 2 MPa, the thermodynamic driving force is seven times higher at 300 °C, leading to the observed enhancement in the reaction rate.
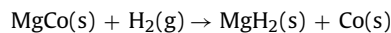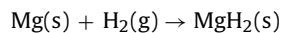
4. Conclusions

Conclusions regarding the formation of MgCo and its influence on the hydriding/dehydriding properties of Mg–Co mixtures are listed below:
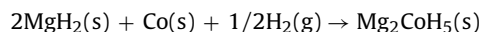
- Formation of MgCo is obtained after Mg_2CoH_5 or $Mg_6Co_2H_{11}$ decomposition only when Mg–Co diffusion is favored by adequate combination of temperature and time. Then, MgCo formation occurs by activated diffusion in the solid-state between Mg–Co.
- Thermal history of Mg–Co mixtures modifies Mg–Co local composition and as a consequence influences both hydriding/dehydriding behavior and the nature of hydride phases produced. The 2Mg–Co mixtures before and after heating at 300 °C during 5 days need to be cycled under hydrogen up to 400 °C to get 2:1 local composition. In opposition, Mg–Co mixture heated at 300 °C during 5 days achieves local homogeneous composition according with the starting mixture. In this last case the formation of Mg_2CoH_5 is favored over others hydrides phases, being the only hydride phase produced. In addition, adequate Co dispersion obtained in the Mg-based matrix acts as catalyst for hydrogen desorption from Mg_2CoH_5 decreasing in more than 100 °C the temperature for hydrogen release.

- The reaction path for the Mg_2CoH_5 formation from Mg–Co mixture present two steps during heating up to 400 °C. It can be represented as follows:
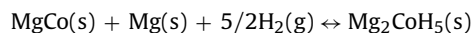
First step, up to 200 °C:

$$Mg(s) + H_2(g) \rightarrow MgH_2(s)$$

$$MgCo(s) + H_2(g) \rightarrow MgH_2(s) + Co(s)$$

Second step, up to 400 °C

$$2MgH_2(s) + Co(s) + 1/2H_2(g) \rightarrow Mg_2CoH_5(s)$$

MgCo compound and MgH_2 hydride are both intermediate phases for the formation of Mg_2CoH_5. The global reaction of Mg_2CoH_5 formation/decomposition can be expressed as

$$MgCo(s) + Mg(s) + 5/2H_2(g) \leftrightarrow Mg_2CoH_5(s)$$

The reversibility of this reaction is possible and depends on temperature and time, at hydrogen pressure fixed, according to thermodynamic information.

- The presence of MgCo compound during isothermal hydriding of Mg–Co mixtures decreases the absorption rate and the total hydrogen storage capacity. Some mass transport step involved in the disproportion reaction of MgCo/MgH_2 seems to control the global reaction rate.

References

[1] A. Züttel, A. Borgschulte, L. Schlapbach (Eds.), Hydrogen as a Future Energy Carrier, Wiley-VCH, Weinheim, 2008.
[2] T. Massalski, H. Okamoto, P. Subramanian, L. Kacprzak (Eds.), Binary Alloy Phase Diagrams, 2nd ed., American Society for Metals, Metals Park, OH, 1990.
[3] P. Zolliker, K. Yvon, P. Fisher, J. Schefer, Inorg. Chem. 24 (1985) 4177–4180.
[4] J.-J. Didisheim, P. Zolliker, K. Yvon, P. Fisher, J. Schefer, M. Gubelmann, A.F. Williams, Inorg. Chem. 23 (1984) 1953–1957.

[5] E.J. Ivanov, I.G. Konstanchuk, A. Stepanov, M. Yan Jie, B. Pezat, Darriet, Inorg. Chem. 28 (1989) 613–615.
[6] R. Černý, F. Bonhomme, K. Yvon, P. Fisher, P. Zolliker, D.E. Cox, A. Hewat, J. Alloys Compd. 187 (1992) 233–241.
[7] P. Selvam, K. Yvon, Int. J. Hydrogen Energy 16 (1991) 615–617.
[8] J. Huot, H. Hayakawa, E. Akiba, J Alloys Compd. 248 (1997) 164–167.
[9] J. Chen, H.T. Takeshita, D. Chartouni, N. Kuriyama, T. Sakai, J. Mat. Sci. 36 (2001) 5829–5832.
[10] R. Varin, S. Li, A. Calka, D. Wexler, J. All. Compd. 373 (2004) 270–286.
[11] S. Li, R.A. Varin, O. Morozova, T. Khomenko, J. All. Compd. 384 (2004) 231–248.
[12] H. Shao, H. Xu, Y. Wang, X. Li, J. Solid State Chem. 177 (2004) 3626–3632.
[13] F. Gennari, F. Castro, J.J. Andrade Gamboa, J. Alloys Compd. 339 (2002) 261–267.
[14] F. Castro y, F.C. Gennari, J. Alloys Compd. 375 (2004) 292–296.
[15] F.C. Gennari, yM.R. Esquivel, J. Alloys Compd. 459 (2008) 425–432.
[16] I. González Fernández, G.O. Meyer, F.C. Gennari, J. Alloys Compd. 446–447 (2007) 106–109.
[17] I. González Fernández, F.C. Gennari, G.O. Meyer, J. Alloys Compd. 462 (2008) 119–124.
[18] I. González Fernández, G.O. Meyer, F.C. Gennari, J. Alloys Compd. 464 (2008) 111–117.
[19] J.A. Puszkiel, P. Arneodo Larochette, F.C. Gennari, J. Alloys Compd. 463 (2008) 134–142.
[20] J.A. Puszkiel, P. Arneodo Larochette, F.C. Gennari, J. Power Sources 186 (2009) 185–193.
[21] M. Yoshida, F. Bonhomme, K. Yvon, P. Fischer, J Alloys Compd. 190 (1993) L45–L46.
[22] F.C. Gennari, F. Castro, J. Alloys Compd. 396 (2005) 182–192.
[23] G. Meyer, D.S. Rodríguez, F. Castro, G. Fernández, Hydrogen Energy Progress, in: Proceedings of the 11th World Energy Conference, Stuttgart, vol. 2, 1996, pp. 1293–1297.
[24] C. Rongeat, I. Llamas.-Jansa, S. Doppiu, S. Deledda, A. Borgschulte, L. Schultz, O. Gutfleisch, J. Phys. Chem. B 111 (2007) 13301–13306.
[25] J.J. Reilly, R.H. Wiswall, Inorg. Chem. 6 (1967) 2220–2223.
[26] N. Hanada, T. Ichikawa, H. Fujii, J. Phys. Chem. B 109 (2005) 7188–7194.
[27] C.T. Hsieh, J.L. Wei, J.Y. Lin, W.Y. Chen, J. Power Sources 183 (2008) 92–97.